Magnetism in orbitally unquenched chainar compounds. I. The antiferromagnetic case: $RbFeBr_3$

M. E. Lines and M. Eibschütz
Bell Laboratories, Murray Hill, New Jersey 07974
(Received 16 December 1974)

Measurements of the quadrupole splitting by the Mössbauer effect and of single-crystal magnetic susceptibility are reported over a wide temperature range for the quasi-linear-chain antiferromagnet $RbFeBr_3$. A magnetic analysis of the Fe^{2+} chains for this orbitally degenerate system using the correlated-effective-field theory is given in terms of only three parameters, a spin-orbit coupling, a crystal-field trigonal distortion, and a Heisenberg exchange J between real spins. We find a nearest-neighbor intrachain exchange energy $-2J\vec{S}_i\cdot\vec{S}_j$, where $J = -2.5 \pm 0.4$ °K. Interchain exchange can be estimated from the observed Néel temperature and is at least an order of magnitude smaller than J. A comparison of the correlated-effective-field approximation with the known exact response for classical Heisenberg linear chains is also presented to indicate the relative accuracy of the method in the linear-chain context.

I. INTRODUCTION

In this and the following paper we attempt to understand the magnetic properties of the chainar compounds $RbFeBr_3$ and $RbFeCl_3$. Although crystallographically very similar, $RbFeBr_3$ forms antiferromagnetic in-chain correlations as the temperature is lowered while $RbFeCl_3$ develops ferromagnetic correlations. This basic difference is reflected in the long-range order, which sets in at very low temperatures; this order being precipitated by very small antiferromagnetic interchain interactions in both cases.

Interest in cooperative phenomena associated with magnetic linear-chain systems has been increasing in recent years (for a review see de Jongh and Miedema[1]) but quantitative theoretical understanding even of static phenomena is still lacking in many cases, particularly in the presence of anisotropy. Difficulties are further compounded if the magnetic ions involved are orbitally unquenched, as is the case for the Fe^{2+} ions in $RbFeBr_3$ and $RbFeCl_3$. A self-consistent formalism then necessitates the inclusion of correlation effects in thermally excited crystal-field levels as well as between the lower single-ion states. Magnetic susceptibility measurements for $RbFeCl_3$ have already been reported in the literature[2] although, as we shall demonstrate below, the published theoretical interpretations[2,3] are in violent conflict and, we believe, are equally untenable, not because of errors of analysis but simply because of the extreme difficulty of the chainar problem in this context and the inadequacy of the approximations assumed.

In this and the following paper, Paper II, we have tried to improve the theoretical situation without in any way claiming to have "solved" the general problem. We have adapted the correlated-effective-field (CEF) theory (developed recently by one of the authors[4]) for use in the orbitally unquenched chainar problem. This theory includes correlations between neighbor spins by adding to the common random-phase effective field an in-phase contribution, the temperature-dependent amplitude of which is completely determined by making the theory obey the fluctuation-dissipation theorem. While it is a significant improvement upon the existing analyses[2,3] and indeed appears to be surprisingly quantitative for the antiferromagnetic bromide situation, of equal importance is the fact that we have been able to carry out a more complete crystal-field analysis than the earlier authors, reducing the number of "free" parameters in the problem quite substantially, and thereby enabling a much more stringent test of theoretical accuracy to be obtained.

$RbFeCl_3$ and $RbFeBr_3$ belong to the hexagonal space group $P6_3/mmc$ (D_{6h}^4).[5-7] The chains lie along the c axis and consist of slightly distorted $(FeX_6)^{4-}$ octahedra (X = Cl, Br) which share their (111) faces; see Fig. 1. The one-dimensional character arises primarily because the $(FeX_3)^-$ chains are widely spaced in the basal plane, the interchain separation being of order 7 Å and more than twice the ~3-Å distance between Fe^{2+} ions within the chains. The Fe^{2+} site symmetry is trigonal $\bar{3}m(D_{3d})$. Below about 120 °K in the bromide a crystallographic transition to a lower symmetry occurs (space group $P6_3cm$).[7] The new unit-cell edges are $a' = a\sqrt{3}$, $c' = c$ in terms of the $P6_3/mmc$ cell and the Fe^{2+} ions occupy two sets of nonequivalent sites. The inequivalency, however, is not sufficient to affect nuclear quadrupole splitting in our Mössbauer experiments and we have neglected it throughout.

In this first paper we study $RbFeBr_3$ since it turns out to be the easier to understand. In Sec.

II we report the experimental Mössbauer-effect and magnetic susceptibility measurements. Section III discusses CEF theory in the simpler context of the isotropic Heisenberg linear chain. This is done in order to take advantage of the existence of accurate theoretical data in the Heisenberg context and to estimate the accuracy of the CEF approximation (in an absolute sense and in comparison with other simple closed forms) in the chainar problem. Section IV develops crystal-field theory for Fe^{2+} in the trigonally distorted octahedral environment of $RbFeCl_3$ or $RbFeBr_3$ in order to develop an effective Hamiltonian for the magnetic calculation. Section V performs the CEF statistical calculation on this Hamiltonian and Sec. VI compares the resulting theoretical curves with the experimental Mössbauer and susceptibility data. Finally Sec. VII summarizes our conclusions as regards $RbFeBr_3$.

II. EXPERIMENT

The compound was prepared by D. E. Cox by careful dehydration and reduction of a solution of Rb_2CO_3 and Fe_2O_3 in dilute hydrobromic acid.[8] Single crystals were grown by Bridgman technique. The crystals have excellent (100) cleavage planes. Powder absorbers for the Mössbauer measurements were made by crushing the single crystals in a dry atmosphere and mixing with boron nitride powder.

The ^{57}Fe Mössbauer spectra were obtained in a standard transmission geometry with a conventional constant-acceleration spectrometer[9] using a ^{57}Co in Pd source. Temperatures of 77.4, 20.3, and 4.2 °K were obtained with a sample holder immersed in a cryogenic liquid. Other temperatures were obtained with the sample holder mounted in a Dewar vacuum space on a "cold finger" connected to the liquid reservoir by a variable thermal resistance. In the latter case temperature was measured by a platinum resistance thermometer[10] mounted near the sample. Fluctuations in the temperature of the platinum resistor during runs of 24 h were always less than 0.05 °K. We estimate a gradient of 0.2 °K across the sample and that the platinum resistor provided a measure of the average sample temperature accurate to ± 0.5 °K. Above 300 °K the absorber was in turn mounted in a special constant-temperature oven controlled by a proportional feedback circuit responsive to one of the chromel-alumel thermocouples on the absorber. The total temperature swing was less than 0.01 °K and the gradient across the absorber was less than 0.05 °K.

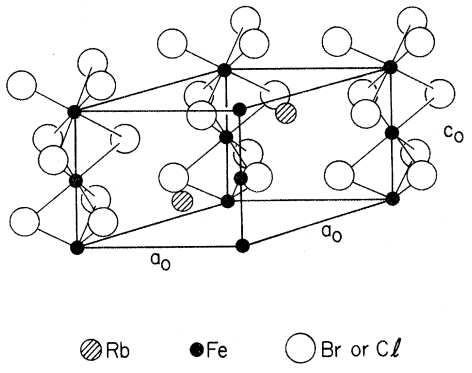

FIG. 1. Unit cell of $RbFeBr_3$ or $RbFeCl_3$.

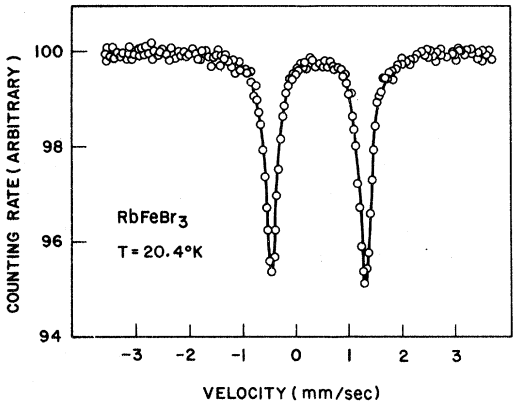

FIG. 2. Representative ^{57}Fe Mössbauer absorption spectrum for powder $RbFeBr_3$. The solid lines are obtained by least-squares fits of the data to sums of Lorentzian curves. The slight asymmetry in the line intensities is possibly due to nonrandom orientation of small single-crystal platelets in the powder sample.

The ^{57}Fe Mössbauer absorption spectra between 1.54 and 400 °K show resonance absorption lines due to the electric field gradient at the iron nucleus. A characteristic spectrum is shown in Fig. 2 and the quadrupole splitting as a function of temperature is shown in Fig. 14 together with a theoretical fit to the data resulting from the calculations set out below.

Magnetic susceptibility single-crystal measurements between 1.5 and 300 °K were taken using a pendulum magnetometer. The resulting curves for $RbFeBr_3$ in a field of 15.3 kOe are shown in Fig. 3, where we also plot reciprocal parallel and perpendicular susceptibilities to demonstrate their linearity above approximately 50 °K.

III. STATISTICAL PROBLEM

For many-body magnetic systems in which unquenched orbital angular momentum plays a major role, quasi-linear chains are perhaps the most difficult to describe in a quantitative fashion. This is essentially because one dimensional systems develop very-long- (but finite) range moment-mo-

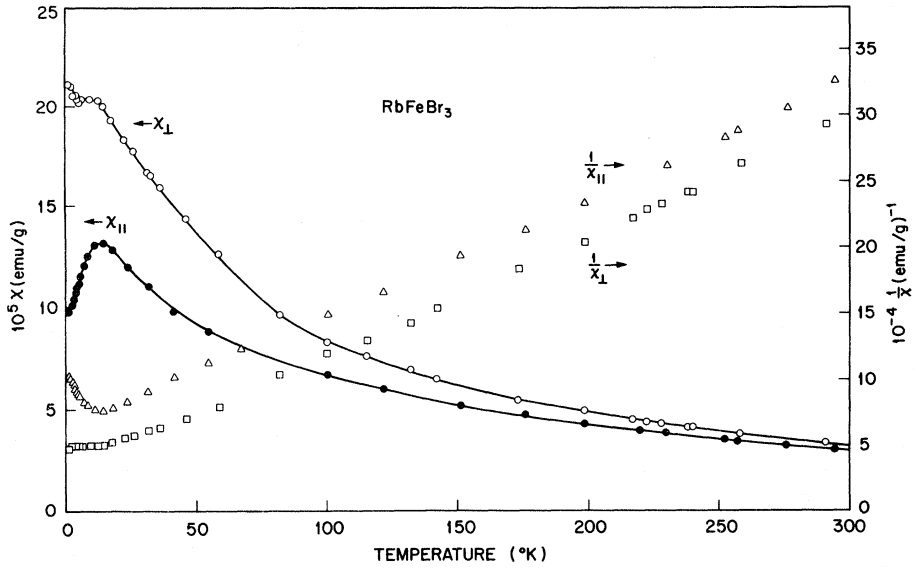

FIG. 3. Single-crystal measurements of magnetic susceptibility parallel and perpendicular to the c axis.

ment correlations as the temperature is lowered and as a result are most poorly described by molecular-field concepts. On the other hand the effects of exchange interactions on thermally excited crystal-field states have traditionally been included in the random-phase (for dynamics) or molecular-field (for statics) approximation, both of which neglect spontaneous fluctuations.

A number of the hexagonal ABX_3-type compounds (where B = Fe or Co, X = Cl or Br) seem to confront us with this problem in a rather severe form for, in addition to being chainar and orbitally unquenched, they may well provide us with examples of non-Heisenberg exchange and some, at least, are singlet-ground-state antiferromagnets. A good example of the difficulties involved is provided by earlier attempts to interpret the magnetic static properties of $RbFeCl_3$ at low temperatures. Representing the system by an anisotropic fictitious spin-1 Hamiltonian and allowing parallel and perpendicular g values to be independent parameters, Achiwa[2] used molecular-field theory to obtain an excellent fit to the low-temperature-susceptibility data with $J_\parallel = -11.5\,^\circ$K, $J_\perp = -3.8\,^\circ$K (both antiferromagnetic), $g_\parallel = 4.73, g_\perp = 4.49$. In an effort to include some measure of fluctuations, Montano *et al.*[3] have analyzed the same curves with the same Hamiltonian but represent the chain by an isolated pair of nearest-neighbor ions: They obtain $J_\parallel \approx 7\,^\circ$K, $J_\perp \approx 16\,^\circ$K (both ferromagnetic), $g_\parallel = 3.52$, $g_\perp = 2.90$. The basic problem is twofold; both approximations are very crude (as we shall demonstrate below) for use in analyzing data in the pertinent low-temperature region, and both model Hamiltonians have far too many "independent" parameters, enabling a convincing fit to the data to be produced almost regardless of the true degree of accuracy of the theory. By performing an adequate crystal-field analysis the number of independent parameters in the problem can be greatly reduced and a much more critical test of theory made possible.

In this paper we shall use the correlated-effective-field (CEF) theory of many-body magnetism set out by Lines[4] to describe systems for which crystal fields, exchange, and thermal energies may all be of comparable magnitude. Before using any statistical approximation in an effort to deduce quantitative parameter information it is useful to understand its strengths and weaknesses at the very outset. To do this we have performed a preliminary analysis of the nearest-neighbor isotropic Heisenberg linear chain of spins for which an *exact* classical solution is known. We calculate in particular the diverging responses of the infinite chain (which corresponds to uniform susceptibility for a ferromagnetic chain or to staggered susceptibility for the antiferromagnet) and compare the molecular-field, isolated-pair-model, and CEF approximations to the exact result.

Fisher's exact solution can be written in the form[11]

$$(\chi_0 J)^{-1} = y[1 - u(y)]/[1 + u(y)], \tag{3.1}$$

in which χ_0 is the susceptibility per spin, and

$$u(y) = \coth(\tfrac{3}{2} y^{-1}) - (\tfrac{2}{3} y) \tag{3.2}$$

with $y = 3kT/4JS(S+1)$. The solution is only truly exact in the limit $S \to \infty$ but is the most accurate closed-form linear-chain approximation available for finite-spin quantum numbers although quantum

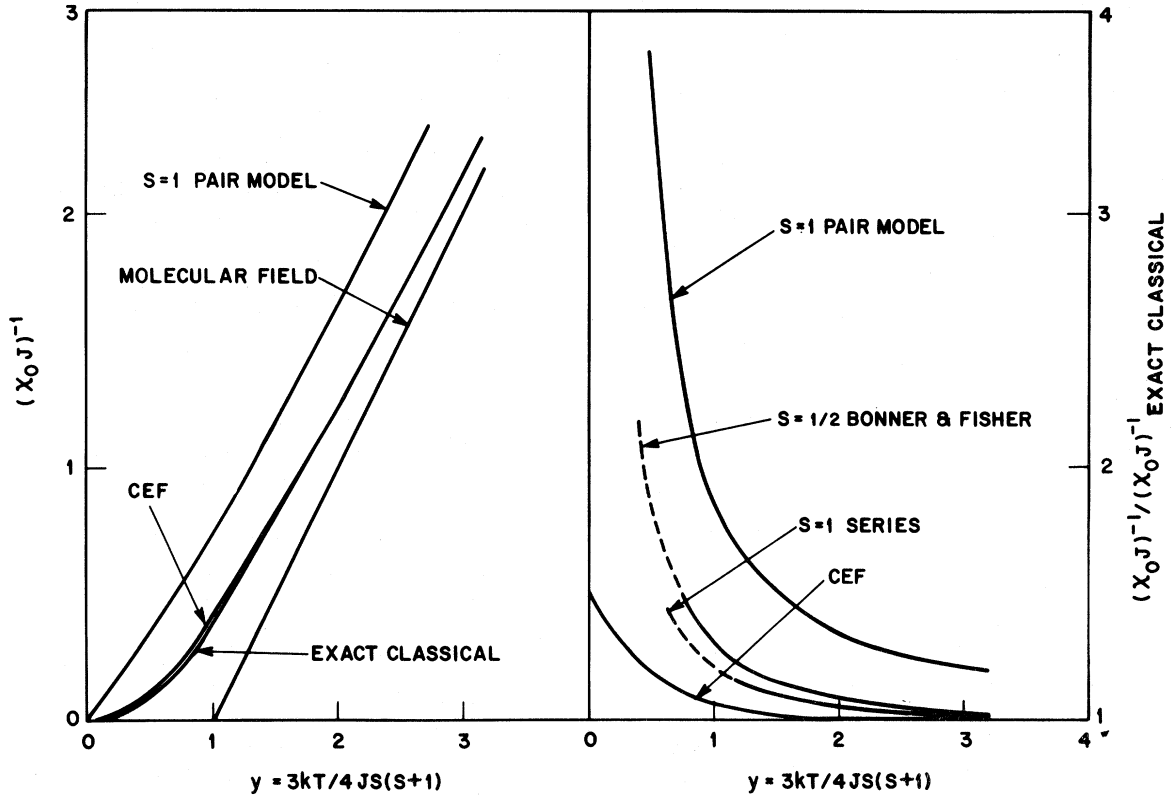

FIG. 4. Reciprocal magnetic susceptibility plotted as a function of temperature for the isotropic Heisenberg ferromagnet in CEF, molecular-field, and spin-1-pair-model approximations and in the exact classical spin limit. On the right-hand side, where the various results are normalized with respect to the exact classical solution, we also plot the best numerical estimates for $S=\frac{1}{2}$, 1 as taken, respectively, from J. C. Bonner and M. E. Fisher [Phys. Rev. 135, A640 (1964)] and from G. S. Rushbrooke and P. J. Wood [Mol. Phys. 1, 257 (1958)].

deviations from (3.1) are far from negligible for $S=\frac{1}{2}$, 1 at low T (see Fig. 4). We define exchange J throughout such that the interaction between nearest neighbors $\vec{S}_i$ and $\vec{S}_j$ is written as $-2J\vec{S}_i \cdot \vec{S}_j$.

The equivalent response in the molecular-field approximation is simply

$$(\chi_0 J)^{-1} = y - 1, \tag{3.3}$$

and in the isolated-pair model is

$$\chi_0 = \frac{\sum_{\frac{2}{3}}^{2} S'(S'+1)(2S'+1)\exp[JS'(S'+1)/kT]}{kT\sum (2S'+1)\exp[JS'(S'+1)/kT]}, \tag{3.4}$$

where the summations run over all values $0, 1, 2, \ldots, 2S-1, 2S$ of the total pair-spin quantum number S'. For the case $S=1$ for which the theory was used by Montano *et al.*,[3] this becomes

$$(\chi_0 J)^{-1} = \frac{y[2+6\,e^{3y^{-1}/4}+10\,e^{9y^{-1}/4}]}{3\,e^{3y^{-1}/4}+15\,e^{9y^{-1}/4}}, \tag{3.5}$$

which has a limiting form $\frac{2}{3}y$ for small y (low temperatures) and $y-\frac{1}{2}$ for large y. Finally, the CEF results is (see Appendix)

$$(\chi_0 J)^{-1} = (1+y^2)^{1/2} - 1. \tag{3.6}$$

These various results are plotted in Fig. 4, where we also include Bonner and Fisher's numerical findings for $S=\frac{1}{2}$ and the high-temperature series estimate for $S=1$. It is immediately apparent that the pair model underestimates the diverging response almost as badly as the molecular-field overestimates it. The CEF approximation slightly overestimates $(\chi_0 J)^{-1}$ for high spin and slightly underestimates it for low spin but is quite evidently a significantly better approximation than the other two. Thus, at $y=1$ (which for Montano's J values corresponds in $RbFeCl_3$ to a temperature of about 30 °K and is a temperature below which much of the pertinent data was taken) the pair model already overestimates $(\chi_0 J)^{-1}$ by more than 50% for $S=1$ while the molecular-field theory has precipitated a spurious long-range order. At this same value of y the CEF estimate for $(\chi_0 J)^{-1}$ deviates from the classical result by +6% and from the less certain $S=1$ result by of order −12%. At still lower temperatures and in particular as $T\to 0$ the only known result of quantitative significance is the exact classical form (3.1). Although quantum deviations may be important in real systems it is

perhaps significant that the CEF and exact classical response have the same diverging form ($\sim A/y^2$) as $y \to 0$ although the CEF amplitude $A=2$ and the exact classical one $A=3$ are different. The pair model on the other hand has a low-temperature response diverging as A/y.

From Fig. 4 it is easy to see how molecular-field theory and the pair model would reach very different conclusions for complex chainar systems if g values were used as free parameters. In this context their low-temperature predictions must be regarded with almost equal skepticism although, judging from the neutron structure determination for $RbFeCl_3$, the pair model is correct in assigning the intrachain exchange a ferromagnetic sign for that case.[6]

IV. CRYSTAL FIELD AND EXCHANGE

In $RbFeBr_3$ the magnetic high-spin ferrous ion sees a quasioctahedral crystal field from its bromine anion neighbors. In the weak-field-coupling scheme the free-ion ground ^5D term is split by the cubic part of the crystal field into an upper orbital doublet and a lower ($^5T_2$) orbital triplet. Within the lower triplet we can make use of the structural isomorphism of the T_2 and P symmetry groups to define a fictitious orbital angular momentum $L'=1$. Within $^5T_2$ the matrix elements of real orbital angular momentum $\vec{L}$ are -1 times the equivalent elements of $\vec{L}'$ within the P states, while the matrix elements of L_z^2 are 3 times those of $L_z'^2$.

Labeling the threefold symmetry (c) axis as the z axis we can write a Hamiltonian representing trigonal distortion from the high octahedral symmetry and spin-orbit interaction in the form

$$\mathcal{H} = \Delta(L_z^2 - 2) + \lambda \vec{L} \cdot \vec{S} , \tag{4.1}$$

where for a free-ion the spin-orbit coupling parameter is $-103\ \mathrm{cm}^{-1}$. In terms of the fictitious angular momentum the Hamiltonian can be rewritten

$$\mathcal{H} = \Delta'(L_z'^2 - \tfrac{2}{3}) + |\lambda|\ \vec{L}' \cdot \vec{S} , \tag{4.2}$$

where $\Delta' = 3\Delta$. It is evident from the susceptibility measurements that z is a hard direction so that, to the extent that the crystal-field anisotropy is the dominant source of magnetic anisotropy, we anticipate a positive value for Δ'. Using the wave-function basis $|M_{L'}, M_S\rangle$ the matrix elements of Hamiltonian (4.2) are readily calculated and the resulting matrix diagonalized as a function of $\Delta'/|\lambda|$ (Fig. 5). For positive values of $\Delta'/|\lambda|$ the ground state is a singlet of the form

$$\psi_0 = a'|1,-1\rangle + b'|0,0\rangle + a'|-1,1\rangle , \tag{4.3}$$

with an excited doublet of form

$$\psi_\pm = a|\pm 1,0\rangle + b|0,\pm 1\rangle + c|\mp 1,\pm 2\rangle , \tag{4.4}$$

a few cm^{-1} higher. The next-higher level is another doublet involving states $|\pm 1, \pm 1\rangle$ and $|0, \pm 2\rangle$ probably distant some 150–250 °K.

Thus, at low temperatures it certainly is valid to represent each ion by its lowest three energy levels. What is most important, however, is the fact that the single parameter $\Delta'/|\lambda|$ determines not only the splitting between ψ_0 and $\psi_\pm$ but both g values as well (apart from possible small orbital-reduction effects). The g values are certainly not free to be used as parameters independent of $\Delta'/|\lambda|$.

In the CEF approximation it is not difficult to retain the entire 15-level structure ($S=2$, $L'=1$) and we do so. The computational difficulties for linear-chain problems of an anisotropic nature arise from the large moment-moment correlations along the chain which perturb the energy levels of Fig. 5 in a temperature-dependent fashion by an amount which reflects the degree of anisotropy and the spin-spin correlation length. Before pursuing the problem in detail it is necessary to give a little thought to the manner in which exchange occurs within the $RbFeBr_3$ chains. Since we are here involved with an orbitally degenerate situation it is certainly not immediately evident that exchange can be written in an isotropic form between real spins. Consider the local symmetry of a nearest-neighbor pair of Fe^{2+} ions in a chain. The ferrous ion has four magnetic holes which, in the Hund's-rule ground state, are divided with two in degenerate ($d\gamma$) e orbitals and two in degenerate ($d\epsilon$) t_2 orbitals. Exchange can occur either by superexchange via the ligand p orbitals, in which case the dominant overlap comes from the $d\gamma$ electrons, or by direct overlap along the c axis via a z lobe $d\epsilon$ orbital.

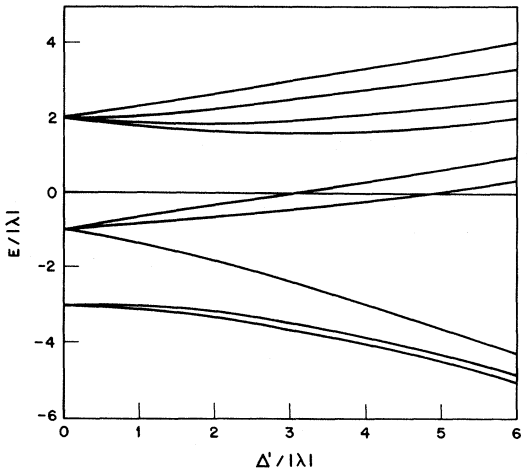

FIG. 5. $^5T_2$ level diagram as a function of the trigonal distortion parameter $\Delta'/|\lambda|$.

Since the orbital degeneracy of e^2 is 1, the superexchange is expected to be of isotropic Heisenberg form. On the other hand the orbital multiplicity of t_2^2 is 3 and the direct exchange will not be of the simple conventional form in an anisotropic environment. Indeed the latter exchange will arise only when the $M_{L'}=0$ orbitals are singly occupied. A direct contribution from $3d$ electrons over a distance of some 3.1 Å would normally be expected to be small compared to σ-bond ligand superexchange, especially via bromine anions, but the situation could be complicated by the fact that the Fe-Br-Fe superexchange angle of 73° is close to that for which the potential and kinetic contributions to superexchange[12] (which are ferromagnetic and antiferromagnetic, respectively) balance (witness the ferromagnetic chainar order in $RbFeCl_3$ with an angle of 75° and the antiferromagnetic chainar order in $RbFeBr_3$ with an angle of 73°). Our philosophy will be to assume the dominance of isotropic exchange, for which the formalism is simplest, and to revise the assumption only if the resulting comparisons of theory with experiment necessitate it.

With Heisenberg exchange between real spins we write an ith-spin Hamiltonian operator

$$\mathcal{H}_i = \Delta'(L_{iz}'^2 - \tfrac{2}{3}) + |\lambda|\vec{L}_i' \cdot \vec{S}_i - \sum_j 2J\vec{S}_i \cdot \vec{S}_j \ , \quad (4.5)$$

where $\sum_j$ runs over the two nearest-neighbor intrachain sites. We assume that interchain interactions are small to the extent that we can neglect them at this stage. We shall verify this assumption later in the paper.

V. CORRELATED-EFFECTIVE-FIELD APPROXIMATION

In the CEF approximation for a paramagnetic phase, and in the initial absence of applied field, the ith-spin Hamiltonian (4.5) is approximated as[4]

$$\mathcal{H}_{eff}^0(i) = \Delta'(L_{iz}'^2 - \tfrac{2}{3}) + |\lambda|\vec{L}_i' \cdot \vec{S}_i + 2J(\alpha_\perp - \alpha_\parallel)S_{iz}^2 \ , \quad (5.1)$$

where $\alpha_\perp$ and $\alpha_\parallel$ are, respectively, measures of nearest-neighbor perpendicular and parallel spin correlations along the chain. More specifically the S_{jz} operator in (4.5) is approximated as $\alpha_\parallel S_{iz}$ and S_{jx} (and S_{jy}) by $\alpha_\perp S_{ix}$ (and $\alpha_\perp S_{iy}$). For isotropic systems the last term in (5.1) vanishes and the perturbational problem of describing the response to an infinitesimal applied field can be performed with correlation-independent zeroth-order wave functions. For our case $\alpha_\perp \neq \alpha_\parallel$ and the zeroth-order wave functions $|n, \alpha\rangle$ are the eigenstates of (5.1) and are temperature dependent since the correlation parameters themselves are temperature dependent. Within the CEF theory the correlations themselves are determined by forcing the theory to obey the fluctuation dissipation theorem. The resulting equations are, for an axially symmetric linear chain [using Eq. (3.17) of Ref. 4],

$$\alpha_\parallel = \frac{\langle \cos\theta / \{t - 4[\cos\theta - \alpha_\parallel]\langle S_z : S_z\rangle\}\rangle_\theta}{\langle 1/\{t - 4[\cos\theta - \alpha_\parallel]\langle S_z : S_z\rangle\}\rangle_\theta} \ , \quad (5.2)$$

$$\alpha_\perp = \frac{\langle \cos\theta / \{t - 4[\cos\theta - \alpha_\perp]\langle S_x : S_x\rangle\}\rangle_\theta}{\langle 1/\{t - 4[\cos\theta - \alpha_\perp]\langle S_x : S_x\rangle\}\rangle_\theta} \ , \quad (5.3)$$

in which the averages $\langle \cdots \rangle_\theta$ are for θ running between 0 and 2π, the parameter $t = kT/J$, and a colon product $\langle A : B\rangle$ is defined as

$$\langle A : B\rangle = \sum_n \rho_n \left(A_{nn}B_{nn} + 2kT \sum_{m \neq n} \frac{A_{nm}B_{mn}}{E_m(\alpha) - E_n(\alpha)} \right) \ , \quad (5.4)$$

where ρ_n is the density matrix

$$\rho_n = e^{-E_n(\alpha)/kT} \Big/ \sum_n e^{-E_n(\alpha)/kT} \ , \quad (5.5)$$

$A_{mn} = \langle m, \alpha | A | n, \alpha\rangle$, etc., and $|n, \alpha\rangle$ and $E_n(\alpha)$ are the eigenfunctions and eigenvalues of Hamiltonian (5.1).

The equations (5.2) and (5.3) are not independent and must be solved simultaneously for the two correlation parameters as functions of temperature. Using the basis states $|M_{L'}, M_S\rangle$ the whole self-consistency problem was programmed for computer. For positive values of $\Delta'/|\lambda|$ the c axis is a hard direction and $\alpha_\perp$ is greater than $\alpha_\parallel$ at all temperatures, the differences $\alpha_\perp - \alpha_\parallel$ increasing monotonically with decreasing temperature. The parallel (to the c axis) correlations, in particular, pass through a maximum as the temperature decreases and fall off to small values as $T \to 0$. In Fig. 6 we plot typical sets of correlation curves for one particular value of $\Delta'/|\lambda|$ and different values of exchange. The curves are plotted for ferromagnetic exchange but it is very simple, with CEF, to establish that for the simple chainar system under consideration (and indeed for any loose-packed magnetic lattice with only nearest-neighbor exchange) a reversal of the sign of J merely reverses the signs of $\alpha_\parallel$ and $\alpha_\perp$ and therefore leaves the final term in (5.1) unchanged.

Uniform static magnetic susceptibility per spin within the CEF approximation is given by Eq. (3.15) of Ref. 4 as

$$kT\chi_0^z = \langle \mu_z : \mu_z\rangle + \frac{4J(1-\alpha_\parallel)\langle \mu_z : S_z\rangle^2}{kT - 4J(1-\alpha_\parallel)\langle S_z : S_z\rangle} \ , \quad (5.6)$$

$$kT\chi_0^x = kT\chi_0^y = \langle \mu_x : \mu_x\rangle + \frac{4J(1-\alpha_\perp)\langle \mu_x : S_x\rangle^2}{kT - 4J(1-\alpha_\perp)\langle S_x : S_x\rangle} \ , \quad (5.7)$$

where $\vec{\mu} = 2\vec{S} + k\vec{L} = 2\vec{S} - k\vec{L}'$ is the magnetic moment operator, k being an orbital-reduction parameter. Once the correlation parameters have been determined, the computation of parallel (χ_0^z) and perpendicular ($\chi_0^x = \chi_0^y$) uniform susceptibility is therefore numerically straightforward and, very significantly, has the relevant g factors already included in a self-consistent manner. The parameters to be determined are only three in number: the spin-orbit coupling constant (whose ratio to the equivalent free-ion value essentially determines the orbital reduction parameter k), the trigonal anisotropy $\Delta'/|\lambda|$, and the exchange J.

VI. COMPARISON WITH EXPERIMENT

The quadrupole splitting in an electric field gradient of axial symmetry contains an orbital contribution from the magnetic electrons on the ion in question and a lattice contribution, the former having a temperature dependence proportional to $\langle L_z^2 - 2\rangle$ (or, equivalently, $\langle L_z'^2 - \frac{2}{3}\rangle$) and the latter being approximately independent of temperature. The relative magnitudes of the two terms cannot be calculated with confidence from first principles at the present time and we shall proceed by fitting an expression $A\langle L_z^2 - 2\rangle + B$ to the experimental splitting, with A and B as adjustable parameters. The first indication that B may be relatively quite large (and of the same sign as A) can be obtained by plotting the experimental results against reciprocal temperature (Fig. 7). Since theoretically $\langle L_z^2 - 2\rangle$ is expected to vary linearly with $1/T$ at high temperatures, we anticipate a linear extrapolation to the vertical axis and, from Fig. 7, a value of $B \sim 0.8$–0.9 mm/sec seems quite possible, which is a lattice contribution of order 50% of the low-temperature splitting.

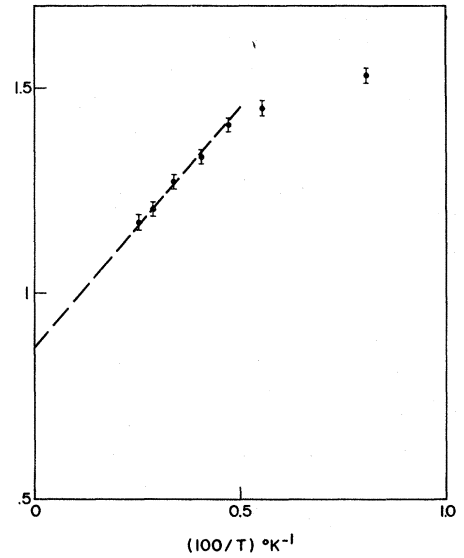

FIG. 7. Experimental values of nuclear quadrupole splitting plotted as a function of reciprocal temperature and extrapolated linearly to $T^{-1} = 0$.

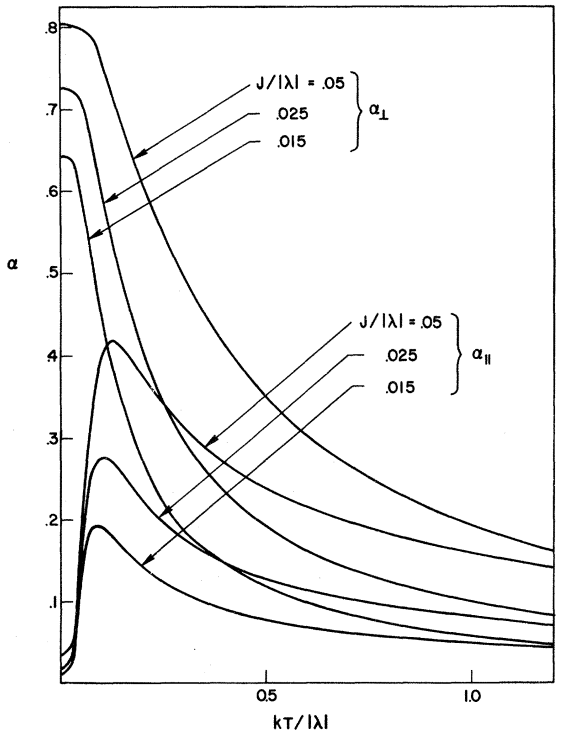

FIG. 6. CEF correlation parameters as functions of temperature for the trigonal distortion $\Delta'/|\lambda| = 1.3$ (which is that found below to be applicable for the case of $RbFeBr_3$) and for various values of interchain exchange. The curves are plotted for ferromagnetic J; changing the sign of J simply changes the sign of α.

Proceeding more quantitatively we can compute $\langle L_z^2 - 2\rangle$ from CEF theory. In the absence of exchange (e.g., the molecular-field result for a disordered phase) the curves as a function of $kT/|\lambda|$ for a series of values of anisotropy $\Delta'/|\lambda|$ are shown in Fig. 8. The effect of exchange is increasingly important as temperature is reduced and raises the curves above their zero-exchange values. However, for exchange energies JS^2 of the order of those found in the hexagonal ABX_3 compounds, the effects on $\langle L_z^2 - 2\rangle$ are negligible above ~100 °K and we therefore fit the experimental quadrupole curves in the 100–400 °K range to the curves of Fig. 8. Within this range all the theoretical curves $0 < \Delta'/|\lambda| \leq 3$ scale with amplitude as a function of $kT/|\lambda|$ and a quantitative fit to experiment can be obtained with the scaled common curve. This fit, shown in Fig. 9, enables us to determine the spin-orbit coupling constant as $|\lambda| = 115 \pm 10$ °K (80 ± 7 cm^{-1}), fixing the orbital reduction parameter as $k = 0.78 \pm 0.07$, and to

deduce the value of lattice quadrupole splitting as $B = 0.74 \pm 0.07$ mm/sec.

Using the values $|\lambda| = 115\ ^\circ\mathrm{K}$ and $k = 0.78$ we can now compute the parallel and perpendicular susceptibilities as a function of only two parameters, $\Delta'/|\lambda|$ and $J/|\lambda|$. The computed curves and comparison with experiment are shown in Fig. 10. The agreement is excellent for

$$J/|\lambda| = -0.024 \pm 0.002, \quad \Delta'/|\lambda| = 1.3 \pm 0.2, \tag{6.1}$$

which is $J = -2.8 \pm 0.4\ ^\circ\mathrm{K}$ (antiferromagnetic).

The relevant parameters are now completely determined and the agreement between theory and experiment for magnetic susceptibility indicates that an isotropic exchange term of Heisenberg form is indeed compatible with experiment for $RbFeBr_3$. However, since the magnetic system orders at $T_N \approx 5.5\ ^\circ\mathrm{K}$ there must be a small but significant contribution to magnetic exchange coming from interchain interactions. Since interchain separation is in excess of 7 Å and occurs via a well-defined two-bromine bridge it is expected to be small (compared to intrachain exchange) and should also be of Heisenberg superexchange character. Although theories for critical temperature in weakly interacting chain lattices are rather crude, even for isotropic S-state magnetic ions, some idea of the magnitude of the interchain exchange (say J') can be obtained by using Oguchi's Green's-function

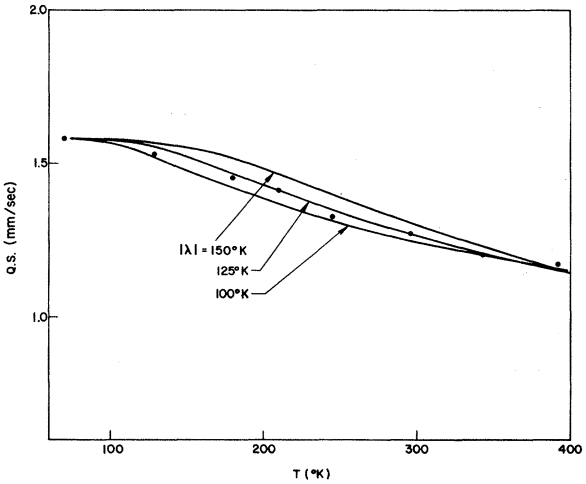

FIG. 9. Fit of the higher-temperature quadrupole splitting data to theory (see text) for different values of the spin-orbit coupling constant.

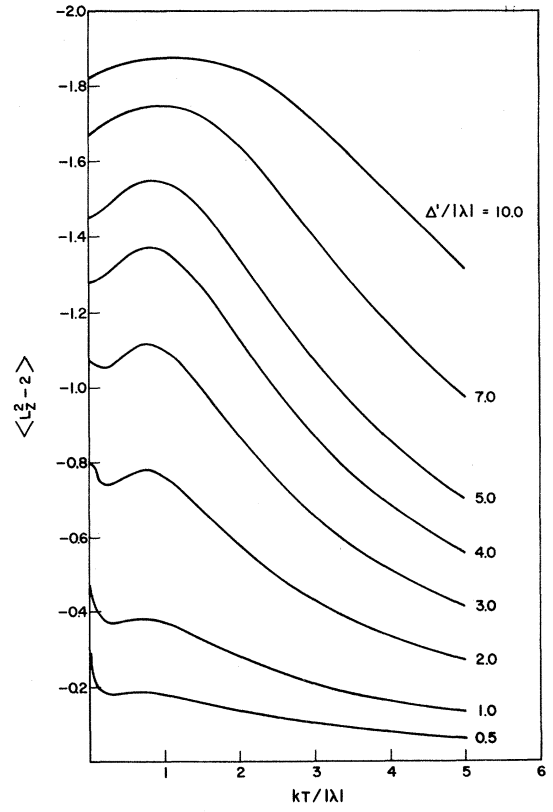

FIG. 8. Ensemble average $\langle L_z^2 - 2 \rangle$ as a function of temperature in the absence of exchange for positive values of distortion parameter $\Delta'/|\lambda|$.

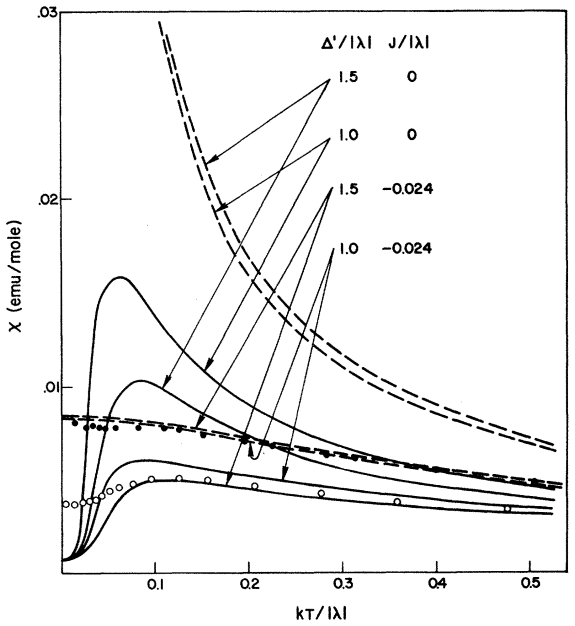

FIG. 10. Curves of the temperature dependence of parallel and perpendicular magnetic susceptibility as calculated in the CEF approximation (with orbital reduction $k = 0.78$ and spin-orbit coupling $|\lambda| = 115\ ^\circ\mathrm{K}$) for different values of distortion $\Delta'/|\lambda|$ and exchange $J/|\lambda|$. Full curves refer to susceptibility parallel to the c axis, dashed curves to a perpendicular direction. The experimental data are indicated by the open circles for $\chi_{\parallel}$ and by closed circles for $\chi_{\perp}$.

estimates.[13] Oguchi's calculation was performed for a loose-packed ensemble of chains, each chain having four nearest-neighbor chains. Thus the ratio of interchain to intrachain exchange fields in the Oguchi calculation is $2J'/J$. In $RbFeBr_3$ the chains are close packed, each chain having six nearest-neighbor chains. On the other hand in the ordered phase the ordering is not the classic up-down two-sublattice antiferromagnetism (since this is not possible for a close-packed antiferromagnet) and the resulting effective interchain field is only half its "saturation" value. Thus in $RbFeBr_3$ the ratio of interchain to intrachain fields in the ordered phase is $3J'/2J$. Oguchi calculates

$$kT_N = 4JS(S+1)/[3I(\eta)], \tag{6.2}$$

where η is $\frac{1}{2}$ times the ratio of the exchange fields (i.e., J'/J for his case) and $I(\eta)$ as a function of η is tabulated.[13] Putting $T_N = 5.5\,^\circ\mathrm{K}$ and $J = 2.8\,^\circ\mathrm{K}$ we find $I(\eta) \approx 4.0$ and $\eta \approx 0.025$. Thus we anticipate for our case a ratio of interchain to intrachain fields of order 0.05, which leads to $|J'/J| \sim 0.03$ or to a value of $|J'| \sim 0.1\,^\circ\mathrm{K}$. From the neutron spin pattern its sign must be negative (antiferromagnetic).

Although this is hardly better than an order-of-magnitude estimate one should perhaps now allow for the fact that the J of Eq. (6.1) is more accurately a measure of total paramagnetic exchange and should therefore be replaced by $J+3J'$. This refines our estimate of exchange to

$$J = -2.5 \pm 0.4\,^\circ\mathrm{K}, \quad J' \approx -0.1\,^\circ\mathrm{K}. \tag{6.3}$$

Since the low-temperature magnetic properties can be adequately described in terms of only the lowest three single-ion energy levels it is perhaps useful to record our findings in the alternative language of a fictitious-spin $S'=1$ effective Hamiltonian. For an anisotropy $\Delta'/|\lambda| \approx 1.3$ the eigenfunctions of the lowest magnetic singlet and the first excited doublet are as given in (4.3) and (4.4), where

$$\begin{aligned} &a' \approx 0.48, \quad b' \approx -0.73, \\ &a \approx 0.34, \quad b \approx -0.68, \quad c \approx 0.65. \end{aligned} \tag{6.4}$$

Within these states the matrix elements of real-spin components $S^\pm$ and S_z are related to those of a fictitious spin S' by

$$S^\pm = Q S'^\pm, \quad S_z = R S'_z, \tag{6.5}$$

where $Q = 1.59$ and $R = 1.30$. For $J = -2.5\,^\circ\mathrm{K}$ this leads to a spin Hamiltonian for intrachain exchange of the form

$$\mathcal{H} = \sum_{i>j} [\,2J_\perp(S'_{ix}S'_{jx} + S'_{iy}S'_{jy}) + 2J_\parallel S'_{iz}S'_{jz}\,], \tag{6.6}$$

where $J_\perp = -Q^2J \approx 6.3\,^\circ\mathrm{K}$ and $J_\parallel = -R^2J \approx 4.2\,^\circ\mathrm{K}$.

Associated with this exchange is a crystal-field splitting (i.e., $+DS'^2_z$) between the gound singlet $|0\rangle$ and excited doublet $|\pm 1\rangle$, where $D \approx 0.11|\lambda| \approx 12-13\,^\circ\mathrm{K}$, and g values $g_\perp \approx 3.6$ and $g_\parallel \approx 2.8$. Finally, and most importantly, the Van Vleck temperature-independent susceptibility in the spin-1 picture is of essential importance and contributes (see $\chi_\parallel$ as $T \to 0$ in Fig. 10) up to 20% of the total susceptibility at intermediate temperatures.

In the spin-1 representation an interesting consistency check can be obtained by noting a rather subtle feature of the experimental perpendicular susceptibility plot. Although barely discernible on the scale of Fig. 10 and completely absent in the CEF theory, there is a weak rounded maximum at $10 \pm 1\,^\circ\mathrm{K}$ in $\chi_\perp$. This is a well-known many-body feature of linear-chain antiferromagnetism and can be described theoretically in the simple chain models by extrapolation from finite-chain results (or exactly for the case of classical spins) although it is usually absent in simple closed-form statistical approximations (Fig. 11). For an isotropic spin-1 linear chain the susceptibility maximum occurs[1] at $kT = 2.70J$. But our system at $10\,^\circ\mathrm{K}$ is evidently quite anisotropic and perhaps closer to an XY model or planar Heisenberg model, with spins constrained close to the XY plane. For these models the perpendicular susceptibility exhibits a rounded maximum at a value of $kT/J_\perp$ which is about $\frac{1}{2}$ of the isotropic value (the ratio is almost exactly $\frac{1}{2}$ for the most thoroughly studied example[1] with spin

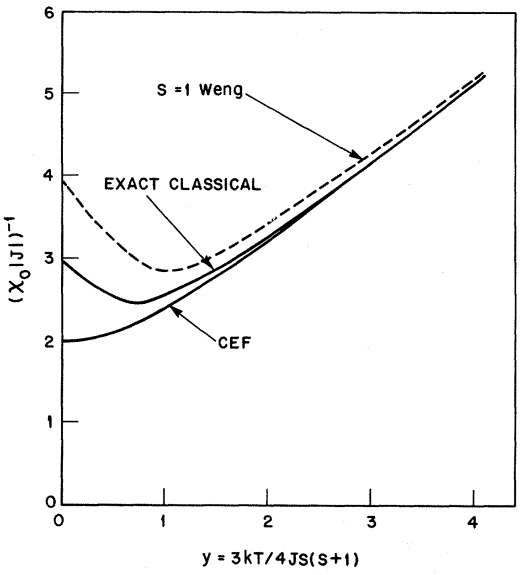

FIG. 11. Comparison of CEF theory and the exact classical result for magnetic susceptibility of an isotropic Heisenberg linear-chain antiferromagnet. Also shown is a numerical estimate for $S=1$ by C. Y. Weng as reported in Ref. 1.

$\frac{1}{2}$). The isotropic and XY models therefore provide us with bounds for $J_\perp$ which, for a susceptibility maximum at 10 °K, are $3.7 < J_\perp < 7.4$ °K, quite consistent with our finding of 6.3 °K. The value 6.3 °K in this context would suggest a model closer to XY than to isotropic at 10 °K and this again would seem to conform qualitatively with our estimate $D \approx 12$–13 °K of crystal-field anisotropy energy. Note that the maximum in parallel susceptibility is not a many-body feature and is well described by simple theories; it is in fact of crystal-field origin and corresponds to the thermal depopulation of the excited doublet level.

Another consistency check (this time a rather quantitative one) can be obtained from the room-temperature anisotropy of susceptibility. Experimentally (Fig. 3) the difference between parallel and perpendicular *reciprocal* susceptibility is closely independent of temperature above about 50 °K and equal to 7.8 ± 0.3 (emu/mole)$^{-1}$. Theoretically we can compute this difference in CEF approximation as a function of $\Delta'/|\lambda|$ and $J/|\lambda|$, and for higher temperatures (see Fig. 12) we find that the difference is dominated by the single parameter $\Delta'/|\lambda|$. Fitting theory with experiment then gives a rather precise measure of crystal-field anisotropy. Neglecting exchange completely gives a value

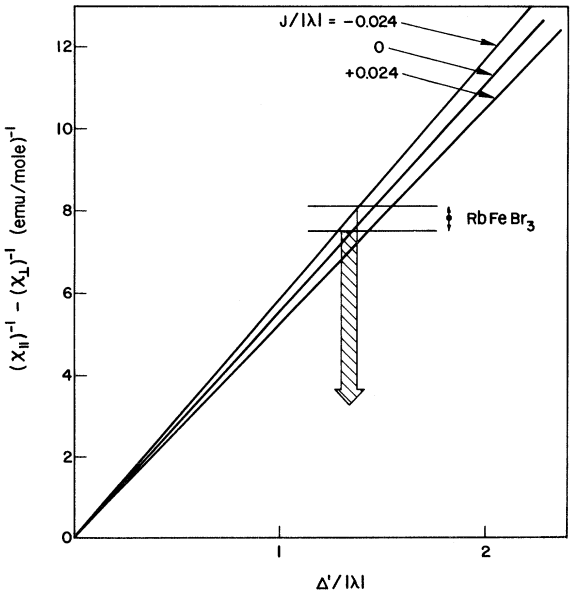

FIG. 12. Theoretical CEF curves of the difference between reciprocal parallel and reciprocal perpendicular susceptibility (calculated with $k = 0.78$, $kT/|\lambda| = 2$) as a function of trigonal distortion $\Delta'/|\lambda|$ for different values of exchange $J/|\lambda|$. The solid circle and error bars mark the constant experimental value taken from Fig. 3 for $T > 50$ °K and the arrow locates the implied value of trigonal distortion $\Delta'/|\lambda| \approx 1.35$.

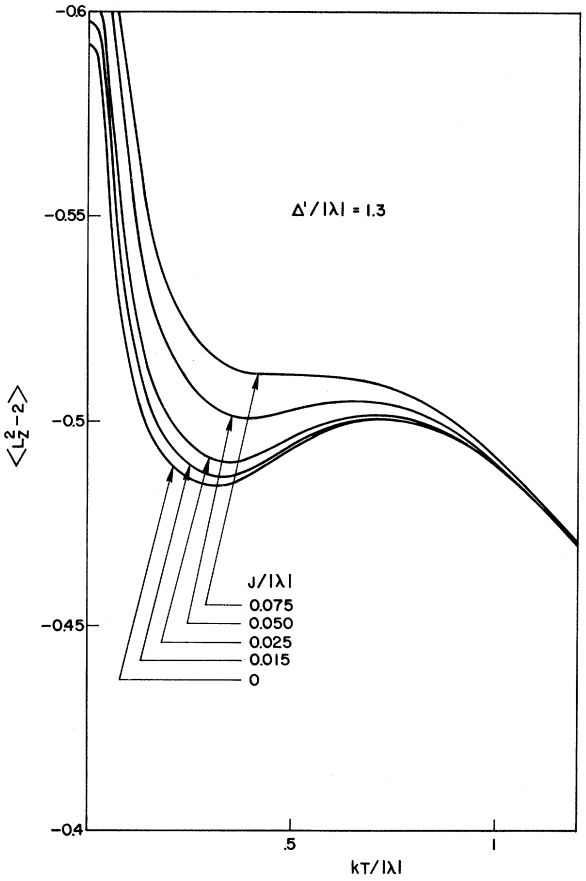

FIG. 13. Ensemble average $\langle L_z^2 - 2\rangle$ as a function of temperature in CEF approximation showing explicitly the effects of intrachain exchange at low temperatures, for the case $\Delta'/|\lambda| = 1.3$.

$\Delta'/|\lambda| = 1.4 \pm 0.05$. Correcting for exchange $J/|\lambda| \approx -0.024$ refines the estimate to $\Delta/|\lambda| = 1.35 \pm 0.05$ and is essentially in exact agreement with the low-temperature finding of (6.1).

Finally we calculate the low-temperature quadrupole splitting for which the presence of exchange and spin correlations modify the earlier zero-exchange calculations of Fig. 8. In Fig. 13 we show the calculated $\langle L_z^2 - 2\rangle$ curves for $\Delta'/|\lambda| = 1.3$ and several different values of exchange. The minimum in the curves becomes shallower as exchange (of either sign) increases and disappears when $J/|\lambda| \approx 0.07$. On the other hand these shifts from the zero-field curves are perhaps the least quantitative of our estimates since they are proportional to the *anisotropy* of correlations (i.e., $\alpha_\perp - \alpha_\parallel$), which is a small and fairly subtle feature of the calculation at intermediate temperatures. The final comparison of theory with experiment for the entire temperature range is shown in Fig. 14. The fit at the lowest temperatures may not be significant since the lowest two experimental points actually

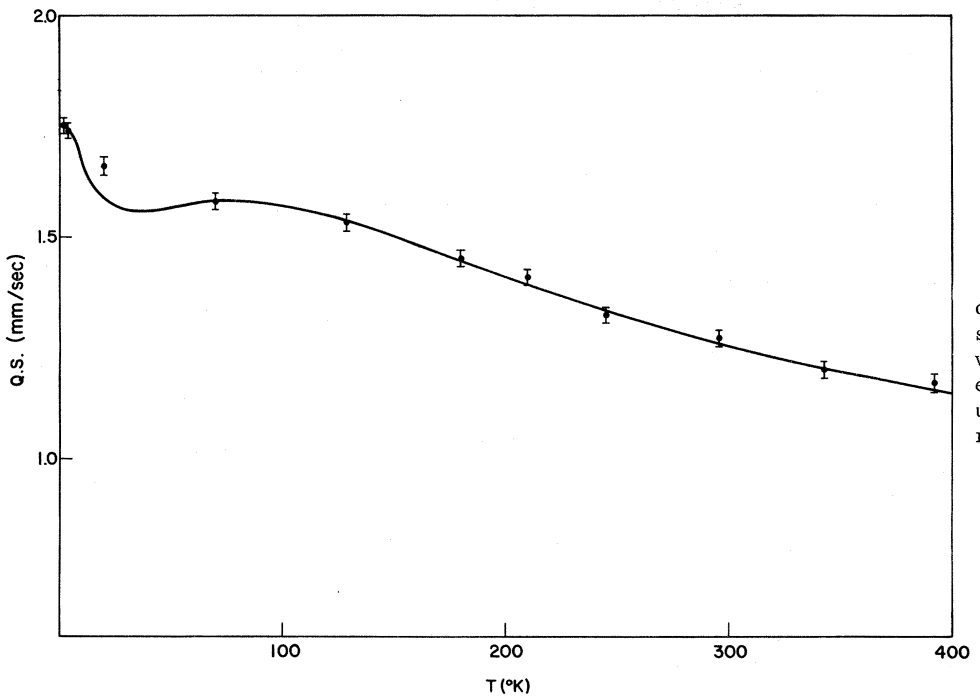

FIG. 14. Comparison of experimental quadrupole splitting (filled circles) with CEF theory over the entire temperature range using the final best-fit parameters.

occur below T_N and an allowance for a modification of the singlet-ground-state wave function and for a splitting of the upper doublet by the long-range order parameter should be made below 5.5 °K. Unfortunately the CEF approximation has yet to be developed for an ordered phase.

Although $RbFeBr_3$ is formally a singlet-ground-state antiferromagnet, the exchange value $J \approx -2.5$ °K is too large compared to crystal-field splitting $D \approx 12$–13 °K for any of the characteristic anomalies associated with classic singlet-ground-state behavior[14] to be much in evidence here. For very small values of $|J|/D$ an ordered phase would not occur. The molecular-field estimate for that critical value of exchange which can just trigger long-range order at $T=0$ is $J_c = D/(8Q^2)$ for the quasi-linear-chain. For our case, Q of Eq. (6.5) is 1.59 and leads to a critical value $|J_c| \approx 0.6$ °K. For $RbFeBr_3$ the estimated $J \approx -2.5$ °K exceeds J_c to a degree which, for example, would make the depression of the Néel temperature by the singlet-ground-state character quite small and render our use of Oguchi theory for estimating interchain exchange at least qualitatively sound.

VII. SUMMARY

$RbFeBr_3$ is a quasi-linear-chain antiferromagnet with $T_N = 5.5$ °K. The unquenched orbital angular momentum of Fe^{2+} leads to markedly anisotropic magnetic properties in the trigonally distorted octahedral local environment of the magnetic cation. We have measured the temperature dependence of the quadrupole splitting at the ion site (by the Mössbauer effect) and also the single-crystal static magnetic susceptibility. The results are interpreted quantitatively in terms of a zero-field linear-chain Hamiltonian

$$\mathcal{H} = \sum_i [\Delta(L_{iz}^2 - 2) + \lambda \vec{L}_i \cdot \vec{S}_i] - \sum_{i>j} 2J \vec{S}_i \cdot \vec{S}_j \qquad (7.1)$$

with only three parameters: a crystal-field distortion Δ, a spin-orbit coupling λ, and an isotropic Heisenberg exchange J between real spins. Using the correlated-effective-field theory of many-body magnetism we obtain quantitative agreement with experiment with $\Delta = 35 \pm 6$ cm^{-1}, $\lambda = -80 \pm 7$ cm^{-1}, and $J = -2.8 \pm 0.4$ °K. The Néel temperature of 5.5 °K can be explained by allowing for the existence of a small interchain exchange $J' \sim -0.1$ °K and, allowing *a posteriori* for its inclusion in the previous analysis, we conclude that the true interchain exchange parameter should more accurately be $J = -2.5 \pm 0.4$ °K. Theoretically the intrachain exchange contains a direct overlap component which is not rigorously of Heisenberg form in addition to the Heisenberg superexchange via the bromine anions. We conclude that any exchange anisotropy introduced by the orbitally degenerate direct contribution is too small to be recognized in the data of this paper. $RbFeBr_3$ is also in principle a singlet-ground-state antiferromagnet, but the exchange $J \approx -2.5$ °K is large compared to the critical value needed to just produce a long-range order at absolute zero to the extent that the marked anomalies characteristic of quasicritical singlet-ground-state systems are likely to be less evident in $RbFeBr_3$.

ACKNOWLEDGMENTS

The authors are grateful to D. E. Cox who supplied the crystals used in this work and to R. C. Sherwood for the performance of the magnetic susceptibility experiments.

APPENDIX

From Eq. (5.7) of Ref. 4 the CEF susceptibility χ_0 for a simple Heisenberg spin-only system with Hamiltonian

$$\mathcal{H} = -\sum_i \sum_j J_{ij} \vec{S}_i \cdot \vec{S}_j \tag{A1}$$

is given by

$$S(S+1)/3kT = \langle 1/\{4\chi_0^{-1} + 2[J(0) - J(\vec{q})]\}\rangle_{\vec{q}}, \tag{A2}$$

where $J(\vec{q})$ is the Fourier transform of exchange J_{ij} with respect to the lattice and $\langle \cdots \rangle_{\vec{q}}$ is an average over the Brillouin zone of the reciprocal lattice. For the specific case of a linear chain with nearest-neighbor-only exchange J this becomes

$$4JS(S+1)/3kT = \langle 1/[(\chi_0 J)^{-1} + 1 - \cos\theta]\rangle_\theta, \tag{A3}$$

where the average over θ runs from $-\pi$ to π. In terms of variables $y = 3kT/4JS(S+1)$ and $\epsilon = (\chi_0 J)^{-1}$ this can be rewritten in the form

$$y^{-1} = \pi^{-1}(1+\epsilon)^{-1} \int_0^\pi \frac{d\theta}{1 - a\cos\theta} = (1+\epsilon)^{-1}(1-a^2)^{-1/2}, \tag{A4}$$

where $a = (1+\epsilon)^{-1}$. Solving explicitly for ϵ we find

$$\epsilon \equiv (\chi_0 J)^{-1} = -1 \pm (1+y^2)^{1/2}. \tag{A5}$$

For a positive J (i.e., ferromagnetic) the positive sign is required and gives immediately the equation (3.6) of the main text.

[1] L. de Jongh and A. R. Miedema, Adv. Phys. 23, 1 (1974).
[2] N. Achiwa, J. Phys. Soc. Jpn. 27, 561 (1969).
[3] P. A. Montano, E. Cohen, H. Shechter, and J. Makovsky, Phys. Rev. B 7, 1180 (1973).
[4] M. E. Lines, Phys. Rev. B 9, 3927 (1974).
[5] H. J. Seifert and K. Klatyk, Z. Anorg. Allg. Chem. 342, 1 (1966).
[6] G. R. Davidson, M. Eibschütz, D. E. Cox, and V. J. Minkiewitz, AIP Conf. Proc. 5, 436 (1971).
[7] M. Eibschütz, G. R. Davidson, and D. E. Cox, AIP Conf. Proc. 18, 386 (1973).
[8] D. E. Cox and F. C. Merkert, J. Cryst. Growth 13/14, 282 (1972).
[9] R. L. Cohen, Rev. Sci. Instrum. 37, 260 (1966); 37, 957 (1966).
[10] Model No. 118L, purchased from Rosemount Engineering Co., Minneapolis, Minn.
[11] M. E. Fisher, Am. J. Phys. 32, 343 (1964).
[12] P. W. Anderson, in *Magnetism*, edited by G. T. Rado and H. Suhl, (Academic, New York, 1963), Vol. I, p. 25.
[13] T. Oguchi, Phys. Rev. 133, A1098 (1964).
[14] R. J. Birgeneau, AIP Conf. Proc. 10, 1664 (1973).